



Research article

Modeling the epidemic trend of middle eastern respiratory syndrome coronavirus with optimal control

Bibi Fatima¹, Mehmet Yavuz^{2,*}, Mati ur Rahman³ and Fuad S. Al-Duais^{4,5}

¹ Department of Mathematics, University of Malakand, Chakadara Dir (Lower), 18800, Khyber Pakhtunkhwa, Pakistan

² Department of Mathematics and Computer Sciences, Faculty of Science, Necmettin Erbakan University, 42090 Konya, Türkiye

³ Department of Computer Science and Mathematics, Lebanese American University, Beirut, Lebanon

⁴ Department of Mathematics, College of Science and Humanities in Al-Aflaj, Prince Sattam bin Abdulaziz University, Al-Aflaj 11942, Saudi Arabia

⁵ Administration Department, Administrative Science College, Thamar University, Thamar, Yemen

* **Correspondence:** Email: mehmetyavuz@erbakan.edu.tr.

Abstract: Since the outbreak of the Middle East Respiratory Syndrome Coronavirus (MERS-CoV) in 2012 in the Middle East, we have proposed a deterministic theoretical model to understand its transmission between individuals and MERS-CoV reservoirs such as camels. We aim to calculate the basic reproduction number (\mathcal{R}_0) of the model to examine its airborne transmission. By applying stability theory, we can analyze and visualize the local and global features of the model to determine its stability. We also study the sensitivity of \mathcal{R}_0 to determine the impact of each parameter on the transmission of the disease. Our model is designed with optimal control in mind to minimize the number of infected individuals while keeping intervention costs low. The model includes time-dependent control variables such as supportive care, the use of surgical masks, government campaigns promoting the importance of masks, and treatment. To support our analytical work, we present numerical simulation results for the proposed model.

Keywords: epidemic model; MERS-CoV; next generation matrix technique; stability analysis; sensitivity analysis; optimal control; numerical simulations

1. Introduction

The coronavirus family comprises a diverse range of viruses that can be found in different animal species, including cats, camels, bats, and cattle. In rare cases, animal coronaviruses can infect humans and spread among them, as has been seen with SARS, MERS, and the current COVID-19 pandemic [1, 2]. Since it first emerged in Saudi Arabia in 2012, the Middle East respiratory syndrome (MERS-CoV) has claimed the lives of 1791 individuals, according to various sources [3, 4]. Meanwhile, the 2003 outbreak of severe acute respiratory syndrome (SARS) resulted in the deaths of 774 individuals [5].

Camels have been identified as the primary carriers of the MERS-CoV virus according to scientific research. Human-to-human transmission is the leading cause of MERS-CoV cases, responsible for 75 to 88 percent of all cases, while the remaining cases are caused by transmission from camels to humans. It is important to note that the virus can spread through respiratory discharge from infected individuals, such as coughing. In addition, close contact, including caring for or living with an infected person, can also result in the transmission of the virus. Since the discovery of MERS-CoV in April 2012, there have been a total of 536 reported cases, with 145 resulting in death. This gives a case fatality rate of 27 percent. The majority of cases have been recorded in the Middle East, specifically in countries such as Saudi Arabia, Jordan, and Qatar, as noted in [6]. It is crucial to maintain awareness of this disease and take appropriate precautions, particularly in areas where the virus has been reported, in order to prevent its spread.

The transmission of MERS-CoV between camels and humans is influenced by various environmental factors. The Hajj and Umrah pilgrimages are significant contributors to the spread of the virus, as these events attract more than 10 million individuals from different parts of the world to Saudi Arabia. Mathematical modeling has proven to be a valuable tool for understanding the outbreak, developing effective control strategies, and exploring the immune response to MERS-CoV. Several modeling studies have been conducted to investigate the MERS-CoV outbreak, as highlighted in [7–9]. One of the most extensive MERS-CoV epidemics was documented by Assire et al. in [10], who provided evidence suggesting that the virus can be transmitted from person to person. The Kingdom of Saudi Arabia (KSA) has reported the highest number of cases, with most of the cases being recorded there. It is imperative to take appropriate measures to mitigate the spread of the virus, especially in areas that have reported cases, in order to prevent further outbreaks. The consumption of unpasteurized camel milk, which is a common practice in KSA, is a potential cause of camel-to-human transmission of MERS-CoV, as suggested by [11]. Furthermore, Poletto et al. have proposed that the movement and mingling of individuals during the Hajj and Umrah events may play a significant role in the spread of MERS-CoV, as noted in [12]. Other activities, such as camel racing and the opening and closing of camel markets, have also been identified as potential contributors to the transmission of MERS-CoV. Several researchers have constructed mathematical models to study various diseases and real-world problems, including MERS-CoV, as mentioned in [13–16]. These models have proven to be useful in predicting the spread of the virus, designing effective control strategies, and exploring the immune response to MERS-CoV. It is important to continue this research in order to better understand the disease and limit its impact on public health.

This study utilizes the next-generation matrix (NGM) approach to model the transmission and spread of MERS-CoV between humans and camels. The researchers calculate the fundamental reproductive number and determine the local stability of the model using the Routh-Hurwitz (RH)

criterion. Furthermore, the global stability of the model is assessed through the Castillo-Chavez and Lyapunov type function methods, and the stability conditions are determined in terms of \mathcal{R}_0 . The parameters that impact the transmission of the disease are analyzed through sensitivity analysis of the fundamental reproductive numbers. On the other hand, there have been numerous effective studies have been conducted related to the modelling of infectious diseases [17–19], their stability analyses [20–22], bifurcation and chaos properties [23–30].

In addition, the study employs an optimal control analysis to minimize the number of infected individuals and increase the number of cured individuals in the community. By identifying the factors that contribute to the spread of MERS-CoV, this research can inform effective control strategies and minimize the impact of the disease on public health.

2. Formulation of the model

In this section, we introduce a transmission model for MERS-CoV that accounts for transmission between people-camel and human-human. The model is formulated using a set of differential equations that describe the dynamics of six distinct population groups. These groups include the susceptible population ($S(t)$), the exposed population ($E(t)$), the symptomatic and infectious population ($I(t)$), the asymptomatic but infectious population ($A(t)$), the hospitalized population ($H(t)$), and the recovered population ($R(t)$). To simplify the modeling process, we make the following four assumptions.

- a. All the parameters and variables are non-negative.
- b. Four transmission routes are considered for the disease transmission, which is from individuals symptomatic to asymptomatic, from which to hospitalize, and then reservoir, which are camels for MERS-CoV.
- c. The rate of death because of MERS-CoV is considered in the compartment that contains the infection.
- d. We suppose two types of recoveries, the first one is natural and the second one is with treatment.

Utilizing the above-considered assumptions, we obtain the non-linear system of ODEs as,

$$\begin{aligned}
 \dot{S}(t) &= \phi - \eta_1 I(t)S(t) - \eta_2 \phi A(t)S(t) - \eta_3 q H(t)S(t) - \eta_4 C(t)S(t) - \varpi_0 S(t), \\
 \dot{E}(t) &= \eta_1 I(t)S(t) + \eta_2 \phi A(t)S(t) + \eta_3 q H(t)S(t) + \eta_4 C(t)S(t) - (\xi + \varpi_0)E(t), \\
 \dot{I}(t) &= \xi \rho E - (\sigma_1 + \sigma_2)I - I(t)(\varpi_0 + \varpi_1), \\
 \dot{A}(t) &= (1 - \rho)\xi E(t) - (\nu + \varpi_0)A(t), \\
 \dot{H}(t) &= \sigma_1 I(t) + \nu A(t) - (\sigma_3 + \varpi_0)H(t), \\
 \dot{R}(t) &= \sigma_2 I(t) + \sigma_3 H(t) - \varpi_0 R(t), \\
 \dot{C}(t) &= \psi_1 I(t) + \psi_2 A(t) - \theta C(t),
 \end{aligned} \tag{2.1}$$

with the initial conditions

$$Ics = \{S(0), I(0), E(0), H(0), A(0), C(0), R(0)\} \geq 0. \tag{2.2}$$

Table 1. The description of control parameters in the considered model (2.1).

Parameter	Description
ϕ	New born ratio
$\eta_1, \eta_2, \eta_3, \eta_4$	Transmission rates
ξ	Progression towards Infected I(t)
σ_1	Hospitalization rate (symptomatic)
σ_2	Recovery rate (without hospitalization)
σ_3	Recovery rate (hospitalized)
θ	Lifetime (Camels)
ψ_1	Virus transmission rate from C(t) (by symptomatic)
ψ_2	Virus transmission rate from C(t) (by asymptomatic)
ν	The rate at which asymptomatic individuals become hospitalized
ϖ_0	The natural death rate
ϖ_1	The death rate due to MERS-CoV
ρ	The rate at which exposed individuals become infected

3. Model well-posedness

Consider, $N_p(t)$ which represents the total population of humans in such a manner that $N_p(t) = E(t) + A(t) + S(t) + I(t) + R(t) + H(t)$, then $N_p(t)$ is bounded with lower bound to be 0 and the upper-bound $\frac{\phi}{\varpi_0}$, i.e., $0 \leq N_p(t) \leq \frac{\phi}{\varpi_0}$.

Using this fact, we present the following theorem:

Theorem 1. If $N_p(t)$ represents the number of human and $0 \leq N_p(t) \leq \frac{\phi}{\varpi_0}$ and $N_p(t) \leq \frac{\phi}{\varpi_0}$, then suggested model (2.1) is well defined in the region as follows:

$$\psi_h = \left\{ (S, I, E, H, A, R, C \in R_+^7, \text{ where } N_p(t) \leq \frac{\phi}{\varpi_0}, C \leq \frac{(\psi_1 + \psi_2)\phi}{\varpi_0} \right\}.$$

Let us adopt \mathbb{B} as Banach space, and positive $u = t_+$, so

$$\mathbb{B} = \varpi^1(0, u) \times \varpi^1(0, u) \times \varpi^1(0, u) \times \varpi^1(0, u) \times \varpi^1(0, u) \times \varpi^1(0, u) \times \varpi^1(0, u), \quad (3.1)$$

where the norm on the space \mathbb{B} is supposed to be as $\|\Pi\| = \sum_{i=1}^7 \|\Pi_i\| = (\Pi_1, \Pi_2, \Pi_3, \Pi_4, \Pi_5, \Pi_6, \Pi_7) \in \mathbb{B}$.

Further, \mathbb{B}_+ represents cone(+ive) of $\varpi^1(0, u)$, so from Eq (3.1), \mathbb{B}_+ is given as

$$\mathbb{B} = \varpi^1(0, u) \times \varpi^1(0, u) \times \varpi^1(0, u) \times \varpi^1(0, u) \times \varpi^1(0, u) \times \varpi^1(0, u) \times \varpi^1(0, u).$$

Hence the state space of system (2.1) yields:

$$\Delta = \left\{ S, I, E, H, A, C, R \in \mathbb{B}_+ \ni 0 \leq N_p(t) \leq \frac{\phi}{\varpi_0}, \right. \\ \left. 0 < S(t) + H(t) + A(t) + R(t) + I(t) \leq \frac{\phi}{\varpi_0}, C \leq \frac{(\psi_1 + \psi_2)\phi}{\varpi_0} \right\}.$$

We suppose an operator which is linear as \mathbf{L} and vector $\psi = (S, I, A, E, H, C, R)$, implies that $\mathbf{L}\psi = (\mathbf{L}_i)^T$, here $i = 1, 2, \dots, 7$ where

$$\begin{aligned}\mathbf{L}_1 &= \left(-\frac{dS}{dt} - \varpi_0 S, 0, 0, 0, 0, 0, 0\right), \\ \mathbf{L}_2 &= \left(0, -\frac{dE}{dt} - (\xi + \varpi_0), 0, 0, 0, 0, 0\right), \\ \mathbf{L}_3 &= \left(0, \xi\rho, -\frac{dI}{dt} - (\sigma_1 + \sigma_2 + \varpi_0 + \varpi_1), 0, 0, 0, 0\right), \\ \mathbf{L}_4 &= \left(0, \xi(1 - \rho), -\frac{dA}{dt} - (\nu + \varpi_0)A, 0, 0, 0, 0\right), \\ \mathbf{L}_5 &= \left(0, 0, \sigma_1, \nu, -\frac{dH}{dt} - (\sigma_3 + \varpi_0)H, 0, 0\right), \\ \mathbf{L}_6 &= \left(0, 0, \sigma_2, 0, \sigma_3, -\frac{dR}{dt} - \varpi_0 R, 0\right), \\ \mathbf{L}_7 &= \left(0, 0, \psi_1, \psi_2, 0, 0, -\frac{dC}{dt} - \theta\right),\end{aligned}$$

and domain $\mathcal{D}(\mathbf{L})$ is

$\mathcal{D}(\mathbf{L}) = \left\{ \phi \in \mathbb{B} : \psi \in \mathbf{LC}[0, u), \phi(0) = I_{cs} \right\}$. Here, $\mathbf{LC}[0, u)$ represent the set containing continuous functions which is defined on the $[0, u)$. Consider \mathcal{O} is the nonlinear operator, that is $\mathcal{O} : B \rightarrow B$ defined as,

$$\mathcal{O}(\psi) = \begin{pmatrix} \phi - \eta_1 IS - \eta_2 \phi AS - \eta_3 qHS - \eta_4 CS \\ \eta_1 IS + \eta_2 \phi AS + \eta_3 qHS + \eta_4 CS \\ 0 \\ 0 \\ 0 \\ 0 \\ 0 \end{pmatrix}. \quad (3.2)$$

Suppose $V(t) = (S(t), I(t), H(t), E(t), A(t), R(t), C(t))$ then the suggested system can be written as

$$\frac{dv}{dt} = \mathbf{L}(V(t)) + \mathcal{O}(V(t)), V(0) \in B,$$

where $V_0 = (I_{cs})^T$. Utilizing the results in [31, 32], we present the existence of the system's (3.2) solution, so we define following theorem:

Theorem 2. For each $V_0 \in B_+$, there arises an interval (maximal) $[0, t_0)$, and unique continuous solution $V(t, V_0)$, in such a way that,

$$V(t) = V(0)e^{\mathbf{L}t} + \int_0^t e^{\mathbf{L}(t-r)} \mathcal{O}(V(\sigma)) d\sigma.$$

Theorem 3. The suggested system (2.1) is invariant (positively) subjected to the non-negative R^7_+ .

Proof. Consider ψ and $h_1 = (\xi + \varpi_0)$, $h_2 = (\sigma_1 + \sigma_2 + \varpi_0 + \varpi_1)$, $h_3 = (\nu + \varpi_0)$, $h_4 = (\sigma_1 + \nu)$, $h_5 = (\theta\varpi_0)$,

$$\frac{d\phi}{dt} = \mathbf{L}\phi + \mathbf{D}.$$

$$\mathbf{L} = \begin{bmatrix} -\varpi_0 & 0 & 0 & 0 & 0 & 0 \\ 0 & -h_1 & 0 & 0 & 0 & 0 \\ 0 & \xi\rho & -h_2 & 0 & 0 & 0 \\ 0 & \xi(1-\rho) & 0 & -h_3 & 0 & 0 \\ 0 & 0 & \sigma_2 & \nu & -h_4 & 0 \\ 0 & 0 & \psi_1 & \psi_2 & 0 & -h_5 \end{bmatrix}, \quad \mathbf{D} = \begin{bmatrix} \phi \\ 0 \\ 0 \\ 0 \\ 0 \\ 0 \end{bmatrix}. \quad (3.3)$$

It could be noted from Eq (3.3), matrix \mathbf{D} is positive, while the off-diagonal of \mathbf{L} are non-negative, so the properties of Metzler type matrix holds. Thus the suggested system is invariant in R^7 . \square

Theorem 4. *We assume a positive initial population value for the problem specified in Eq (2.2) and, if the solutions to the model in Eq (2.1) exist, they will be positive for all u.*

Proof. Let us consider the first equation

$$\frac{dS}{dt} = \phi - \eta_1 I(t)S(t) - \eta_2 \phi A(t)S(t) - \eta_3 q H(t)S(t) - \eta_4 C(t)S(t) - \varpi_0 S(t). \quad (3.4)$$

By constant formula of alternation, we obtain the solution (3.4),

$$\begin{aligned} S(t) &= S(0) \exp[-dt - \int (\eta_1 I(t)S(t) - \eta_2 \phi A(t)S(t) - \eta_3 q H(t)S(t) - \eta_4 C(t)S(t))] dx \\ &+ \phi \exp[-dt - \int (\eta_1 I(t)S(t) - \eta_2 \phi A(t)S(t) - \eta_3 q H(t)S(t) - \eta_4 C(t)S(t))] dx \\ &\times [dt + \int (\eta_1 I(t)S(t) + \eta_2 \phi A(t)S(t) + \eta_3 q H(t)S(t) + \eta_4 C(t)S(t))] dx. \end{aligned}$$

\square

$S(t) > 0$, in the same pattern one can present that, the remaining equations in (2.1) are positive.

4. Stability analysis

The main focus of our study is to examine the mathematical and biological plausibility of the system described in Eq (2.1). To achieve this, we carry out a qualitative analysis of the system dynamics. Initially, we compute the threshold parameter \mathcal{R}_0 , which is commonly referred to as the basic reproduction number. This metric allows us to evaluate the inherent capacity of the disease to spread, and determine whether or not an epidemic will persist or eventually fade out. Additionally, we investigate the equilibria of the system and discuss the factors that lead to system stability.

4.1. Equilibria and basic reproductive number

In this study, we have performed a qualitative analysis of the suggested system in order to identify the conditions under which it remains stable. To achieve this, we have calculated the equilibria of the mathematical model described in Eq (2.1).

One of the most important equilibrium points for this system is the disease-free equilibrium (DFE), which represents the state of the system when no disease is present. In order to determine the DFE point for the system, we equate the right-hand side of the equations to zero, with the exception of the susceptible class S , which we set to its initial value S_0 . By doing so, we are able to obtain the DFE point, which we denote as \mathcal{D}_0 . This point represents an important baseline for the system, against which we can compare the behavior of the system in the presence of disease.

Overall, our qualitative analysis of the suggested system has allowed us to gain a deeper understanding of its behavior under various conditions, including the DFE point which is a key reference point for the system.

$$\mathcal{D}_0 = \left(\frac{\phi}{\varpi_0}, 0 \right).$$

We utilize linear stability to study the dynamics of the DFE point and calculate the condition if the equilibrium point turns towards stability and the model becomes under control.

The endemic equilibrium (EE) point is expressed by $\mathcal{D}_1 = (S^*, E^*, I^*, A^*, H^*, R^*, C^*)$, and it occurs in the presence of disease

$$\begin{aligned} S^* &= \frac{\phi(\nu + \varpi_0)\xi\rho + (\sigma_3 + \varpi_0)Q}{((\eta_1 + \nu(1 - \rho)(\sigma_1 + \sigma_2 + \varpi_0))\varpi_2)}, \\ E^* &= \frac{(\sigma_1 + \sigma_2 + \varpi_0)(Q_1)}{(\xi\rho)(\sigma_3 + \varpi_0)Q} I^*, \\ I^* &= \frac{\xi(1 - \rho)(\sigma_1 + \sigma_2 + \varpi_0)(\mathcal{R}_0 - 1)}{(\nu + \varpi_0)\nu\rho}, \\ A^* &= \frac{\eta_2\phi\xi(1 - \rho)(\sigma_1 + \sigma_2 + \varpi_0)}{(\nu + \varpi_0)\xi\rho Q_2} I^*, \\ H^* &= \frac{\sigma_1(\nu + \varpi_0)(1 - \rho)(\mathcal{R}_0 - 1)}{(\sigma_3 + \varpi_0)(\xi + \varpi_0)\nu} I^*, \\ R^* &= \frac{\sigma_2(\sigma_3 + \varpi_0)(\nu + \varpi_0)\xi + \sigma_1 Q I^*}{(\sigma_3 + \varpi_0)(\nu + \varpi_0)}, \\ C^* &= \frac{\psi_1(\nu + \varpi_0)\xi\rho I^* + \psi_2\xi(1 - \rho)(\mathcal{R}_0 - 1)}{(\nu + \varpi_0)\xi\rho}. \end{aligned}$$

The above equations present that, EE of the model (2.1) exists only, if \mathcal{R}_0 is greater than one. Thus we state the following theorem.

Theorem 5. *The EE point $\mathcal{D}_1 = (S^*, E^*, I^*, A^*, H^*, R^*, C^*)$ exists only in case \mathcal{R}_0 is greater than one.*

The definition of (\mathcal{R}_0) can be described as the number of individuals who become infected after being in contact with an infected individual in a population that is initially fully susceptible and without any prior infections. If $\mathcal{R}_0 > 1$, it means that an epidemic is likely to occur, while if $\mathcal{R}_0 < 1$, an outbreak is unlikely. The value of \mathcal{R}_0 is crucial in determining the strength of control measures that need to be

implemented to contain the epidemic. In order to calculate \mathcal{R}_0 for the suggested model (2.1), we use the method described in [33], we have

$$\mathcal{F} = \begin{bmatrix} 0 & \eta_1 S_0 & \eta_2 \phi S_0 & \eta_3 q S_0 & \eta_4 S_0 \\ 0 & 0 & 0 & 0 & 0 \\ 0 & 0 & 0 & 0 & 0 \\ 0 & 0 & 0 & 0 & 0 \\ 0 & 0 & 0 & 0 & 0 \end{bmatrix},$$

$$\mathcal{V} = \begin{bmatrix} b_1 & 0 & 0 & 0 & 0 \\ -\xi \rho & b_2 & 0 & 0 & 0 \\ b_3 & 0 & b_4 & 0 & 0 \\ 0 & -\sigma_1 & -\nu & b_5 & 0 \\ 0 & -\psi_1 & -\psi_2 & 0 & \varpi_2 \end{bmatrix},$$

where $b_1 = (\xi + \varpi_0)$, $b_2 = (\sigma_1 + \sigma_2 + \varpi_0 + \varpi_1)$, $b_3 = -\xi(1 - \rho)$, $b_4 = (\nu + \varpi_0)$, $b_5 = (\sigma_3 + \varpi_0)$. \mathcal{R}_0 represents spectral-radius of NGM $\bar{H} = \mathcal{F}\mathcal{V}^{-1}$.

So \mathcal{R}_0 for model (2.1) is

$$\mathcal{R}_0 = \frac{\eta_1 \xi \rho S_0}{Q} + \frac{\eta_2 \phi S_0 (1 - \rho)}{(\nu + \varpi_0)(\xi + \varpi_0)} + \frac{\eta_3 q S_0 Q_1}{(\nu + \varpi_0)(\sigma_3 + \varpi_0)Q} + \frac{\eta_4 S_0 Q_2}{\varpi_2 (\nu + \varpi_0)Q}, \quad (4.1)$$

where

$$\begin{aligned} Q &= (\xi + \varpi_0)(\sigma_1 + \sigma_2 + \varpi_0 + \varpi_1), \\ Q_1 &= \xi \varpi_0^2 \psi_2 - \xi \sigma_1^2 \varpi_2 - \xi \sigma_1 \sigma_2 \varpi_2 - \xi \sigma_1 \varpi_0 \varpi_2 - \xi \sigma_1 \varpi_1 \varpi_2 + \xi \sigma_1 \sigma_3 \psi_2 + \xi \sigma_2 \sigma_3 \psi_2 + \xi \sigma_1 \varpi_0 \psi_2 + \xi \sigma_2 \varpi_0 \psi_2 \\ &\quad + \xi \sigma_3 \varpi_0 \psi_2 + \xi \sigma_3 \varpi_1 \psi_2 + \xi \varpi_0 \varpi_1 \psi_2 + \rho \xi \sigma_1^2 \varpi_2 + \xi \rho \varpi_0^2 \psi_2 + \nu \rho \xi \sigma_3 \psi_1 + \nu \rho \xi \varpi_0 \\ &\quad + \xi \rho \sigma_1 \sigma_2 \varpi_2 + \xi \rho \sigma_1 \varpi_1 \varpi_2 - \xi \rho \sigma_1 \sigma_3 \psi_2 - \xi \rho \sigma_2 \sigma_3 \psi_2 - \xi \rho \sigma_1 \varpi_0 \psi_2 + \xi \rho \sigma_3 \varpi_0 \psi_1 \\ &\quad - \xi \rho \sigma_3 \varpi_0 \psi_2 - \xi \rho \sigma_3 \varpi_1 \psi_2 - \xi \rho \varpi_0 \varpi_1 \psi_2, \\ Q_2 &= \eta_4 S_0 (\xi \psi_2 \sigma_2 + \xi \psi_2 \sigma_1 + \xi \psi_2 \varpi_0 + \nu \xi \rho \psi_1 - \xi \rho \psi_2 \sigma_2 - \xi \rho \psi_2 \sigma_1 + \xi \rho \psi_1 \varpi_0 - \xi \rho \psi_2 \varpi_0). \end{aligned}$$

The \mathcal{R}_0 of this model is composed of four components: transmission from individuals who are symptomatic to those who are asymptomatic, transmission from asymptomatic individuals to those who require hospitalization, transmission from hospitalization to the reservoir (camels for MERS-CoV), and transmission from the reservoir to susceptible individuals. These four modes of transmission collectively determine the risk of disease spread during this epidemic.

We study the dynamics of the proposed system (2.1) at DFE with aid of Theorem 6 as follows:

Theorem 6. *The DFE point $\mathcal{D}_0 = (S_0, I_0, E_0, H_0, A_0, C_0, R_0)$, is asymptotically stable (locally) if $\mathcal{R}_0 \leq 1$.*

Proof. The Jacobian-matrix of the model at DFE point $(D_0, 0, 0, 0, 0, 0)$, is:

$$J_0 = \begin{pmatrix} -\varpi_0 & 0 & -\eta_1 S & -\eta_2 \phi S & -\eta_3 q S & -\eta_4 S \\ 0 & -(\xi + \varpi_0) & \eta_1 S & \eta_2 \phi S & \eta_3 q S & \eta_4 S \\ 0 & \xi \rho & -(\sigma_1 + \sigma_2 + \varpi_0 + \varpi_1) & 0 & 0 & 0 \\ 0 & \xi(1 - \rho) & 0 & -(\nu + \varpi_0) & 0 & 0 \\ 0 & 0 & \sigma_1 & \nu & -(\sigma_3 + \varpi_0) & 0 \\ 0 & 0 & \psi_1 & \psi_2 & 0 & -\varpi_2 \end{pmatrix}. \quad (4.2)$$

Characteristic equation of Jacobian matrix (4.2) is:

$$(\zeta + \varpi_0)(\delta + \zeta)(a_1 \zeta^3 + \zeta^4 + a_2 \zeta^2 + a_4 + a_3 \zeta) = 0, \quad (4.3)$$

where

$$\begin{aligned} a_1 &= \sigma_1 + \sigma_2 + \nu \varpi_0 + \sigma_3 \varpi_0 \nu, \\ a_2 &= \sigma_2 + \varpi_0 + \xi \varpi_0 \sigma_1 (1 - \mathcal{R}_0), \\ a_3 &= 2\varpi_0^2 + \sigma_1 + \sigma_2 + \sigma_3 + \varpi_0 + \nu \sigma_1 + \sigma_3 + \sigma_1 \varpi_0 + \sigma_1 \xi + \xi(1 - \rho) + \xi \nu, \\ a_4 &= \eta_3 q S \xi(1 - \rho) + \xi \nu \sigma_1 + \varpi_0 \xi(1 - \rho) \sigma_1 \eta_3 S q \varpi_0 \nu \rho. \end{aligned}$$

$a_1 a_3 a_2 > a_2^2 a_4 + a_2^2$ if $\mathcal{R}_0 < 1$. By RH criteria the real parts of all the roots for characteristic polynomial $P(\zeta)$ are negative, which shows that D_0 is asymptotically local stable [34, 35]. \square

4.2. Global stability analysis

The upcoming proof presents the global stability at DFE point D_0 . To analyze the global stability analysis at F_0 we introduce the Lyapunov function as follows.

Theorem 7. *When the reproductive number \mathcal{R}_0 is less than 1, the disease-free equilibrium of the system is globally and asymptotically stable.*

Proof. Consider the Lyapunov function as

$$U(t) = \frac{1}{2}[(S - S^0) + E(t) + I(t) + A(t) + H(t) + (C - C_0)]^2 + [d_1 S(t) + d_2 E(t) + d_3 A(t) + d_4 H(t) + d_5 C(t)]. \quad (4.4)$$

Here d_i for $i = 1, 2, 3, 4, 5$ are arbitrary constants, to be considered after differentiating Eq (4.4), and using (2.1), so we obtain

$$U'(t) = [(S - S^0) + E + A + I + H + (C - C_0)][\phi - \varpi_0 N_p(t) + \psi_1 I + \psi_2 A - \varpi_2 C + Q Q_1 (\phi - (1 - \mathcal{R}_0) - \varpi_0 E(t))].$$

By considering the +ive parameter $d_1 = d_2 = d_3 = Q Q_1$, $d_4 = \frac{1}{Q_2}$, $d_5 = \varpi_0$ and after the interpretation we obtain

$$\mathfrak{U}'(t) = -[(S - S^0) + E + I + A + H + (C - C_0)][\varpi_0 (\phi - N_p(t)) - \psi_1 I \psi_2 A - \varpi_2 \mathfrak{W}]$$

$$- \mathbb{Q}\mathbb{Q}_1(\phi - (1 - \mathcal{R}_0) - \varpi_0 E(t))],$$

where

$$F^0 = \frac{bN}{\varpi_0}.$$

$\mathcal{U}'(t)$ is negative when $S > S^0$ and $\mathcal{R}_0 < 1$ and $\mathcal{U}'(t) = 0$ in case if $S = S^0$ by the LaSalle's invariance principle [36,37], and $E = A = I = H = C = 0$. Thus the DFE is globally asymptotic stable in F_0 . \square

Theorem 8. *If the threshold value is greater than 1, then the model (2.1) around EE point \mathcal{D}_1 is locally as well as globally asymptotically stable.*

Proof. The linearization of model (2.1) around EE point \mathcal{D}_1 is,

$$J_0 = \begin{pmatrix} A & 0 & -\eta_1 S^* & -\eta_2 \phi S^* & -\eta_3 q S^* & -\eta_4 S^* \\ A_1 & -(\xi + \varpi_0) & \eta_1 S^* & \eta_2 \phi S^* & \eta_3 q S^* & \eta_4 S^* \\ 0 & \xi \rho & -A_1 & 0 & 0 & 0 \\ 0 & \xi(1 - \rho) & 0 & -(\nu + \varpi_0) & 0 & 0 \\ 0 & 0 & \sigma_1 & \nu & -A_2 & 0 \\ 0 & 0 & \psi_1 & \psi_2 & 0 & -\varpi_2 \end{pmatrix},$$

where

$$\begin{aligned} A &= \eta_1 I^* + \eta_2 \phi^* A^* + \eta_3 q H^* + \eta_4 S^*, \\ A_1 &= (\sigma_1 + \sigma_2 + \varpi_0), \\ A_2 &= (\sigma_3 + \varpi_0). \end{aligned}$$

Using row transformation, we obtain:

$$J_0 = \begin{pmatrix} -A & 0 & -\eta_1 S^* & -\eta_2 \phi S^* & -\eta_3 q S^* & -\eta_4 S^* \\ 0 & -\mathfrak{B} & -\eta_1 S^* & -\eta_2 \phi S^* & -\eta_3 q S^* & -\eta_4 S^* \\ 0 & 0 & -\mathfrak{B}_1 & -\eta_2 \phi S^* & -\eta_3 q S^* & -\eta_4 S^* \\ 0 & 0 & 0 & -\mathfrak{B}_2 & -\eta_3 q S^* & -\eta_4 S^* \\ 0 & 0 & 0 & 0 & -\mathfrak{B}_3 & 0 \\ 0 & 0 & 0 & 0 & 0 & -\mathfrak{B}_4 \end{pmatrix}, \quad (4.5)$$

where $\mathfrak{B} = (\xi + \varpi_0)(\eta_1 I^* + \eta_2 \phi A^* + \eta_3 q H^* + \eta_4 S^*)$, $\mathfrak{B}_1 = (\sigma_1 + \sigma_2 + \varpi_0 + \varpi_1)(\xi + \varpi_0)A^*$, $\mathfrak{B}_2 = (\nu + \varpi_0)(\xi + \varpi_0)(\mathcal{R}_0 - 1)A^*$, $\mathfrak{B}_3 = (\sigma_1 + \sigma_2 + \varpi_0 + \varpi_1)(\sigma_3 + \varpi_0)$, $\mathfrak{B}_4 = \varpi_2 \xi \rho (\sigma_1 + \sigma_2 + \varpi_0 + \varpi_1)$.

$$\Xi_1 = -A < 0, \Xi_2 = -\mathfrak{B} < 0,$$

$$\Xi_3 = -\mathfrak{B}_1 < 0, \Xi_4 = -\mathfrak{B}_2 < 0,$$

$$\Xi_5 = -\mathfrak{B}_3 < 0, \Xi_6 = -\mathfrak{B}_4 < 0.$$

When $\mathcal{R}_0 > 1$ the real parts of eigenvalues are negative, hence the model (2.1) is asymptotically locally stable at \mathcal{D}_1 [38]. \square

Theorem 9. If \mathcal{R}_0 is greater than 1, then EE point D_1 is globally asymptotically stable and is not stable if less than 1.

Proof. In order to show the asymptotic global stability of the considered model (2.1) at EE point D_1 , we utilize the Castillo-Chavez technique [39,40]. Now let us take the sub-system of (2.1),

$$\begin{aligned}\frac{dS(t)}{dt} &= \phi - \eta_1 IS - \eta_2 \phi AS - \eta_3 qHS - \eta_4 CS - \varpi_0 S, \\ \frac{dE(t)}{dt} &= \eta_1 IS + \eta_2 \phi AS + \eta_3 qHS + \eta_4 CS - (\xi + \varpi_0)E, \\ \frac{dI(t)}{dt} &= \xi \rho E - (\sigma_1 + \sigma_2)I - (\varpi_0 + \varpi_1)I.\end{aligned}\quad (4.6)$$

Consider \mathcal{P} and $\mathcal{P}^{[2]}$ be the linearized matrix and second-additive of the model which contains the first three equations of system (2.1), which becomes

$$P = \begin{pmatrix} -\delta_{11} & 0 & -\delta_{13} \\ \delta_{21} & \delta_{22} & \delta_{23} \\ 0 & 0 & -\delta_{33} \end{pmatrix}, \quad P^{[2]} = \begin{pmatrix} -(\delta_{11} + \delta_{22}) & \delta_{23} & -\delta_{13} \\ \delta_{32} & -(\delta_{11} + \delta_{33}) & \delta_{12} \\ -\delta_{31} & \delta_{21} & -(\delta_{22} + \delta_{33}) \end{pmatrix}. \quad (4.7)$$

Let $Q(\chi) = Q(S(t), E(t), I(t)) = \text{diag} \left\{ \frac{S}{E}, \frac{S}{E}, \frac{S}{E} \right\}$, then $Q^{-1}(\chi) = \text{diag} \left\{ \frac{E}{S}, \frac{E}{S}, \frac{E}{S} \right\}$, the derivative of $Q_f(\chi)$ w.r.t time, implies that

$$Q_f(\chi) = \text{diag} \left\{ \frac{\dot{S}}{E} - \dot{E} \frac{S}{E^2}, \frac{\dot{S}}{E} - \dot{E} \frac{S}{E^2}, \frac{\dot{S}}{E} - \frac{S\dot{E}}{E^2} \right\}. \quad (4.8)$$

Now $Q_f Q^{-1} = \text{diag}\{K_1, K_1, K_1\}$ and $Q \mathcal{P}_2^{[2]} Q^{-1} = \mathcal{P}_2^{[2]}$, where $K_1 = \dot{S}S - \frac{\dot{E}}{E} \mathbf{A} = Q_f Q^{-1} + Q \mathcal{P}_2^{[2]} Q^{-1}$, and

$$\mathbf{A} = \begin{pmatrix} \mathbf{A}_{11} & \mathbf{A}_{12} \\ \mathbf{A}_{21} & \mathbf{A}_{22} \end{pmatrix}, \quad (4.9)$$

$$\mathbf{A}_{11} = \frac{\dot{S}}{S} - \frac{\dot{E}}{E} - \eta_1 I - \eta_2 \phi A - \eta_3 qH - (\nu + \varpi_0),$$

$$\mathbf{A}_{12} = \begin{bmatrix} \eta_1 S & \eta_2 S \end{bmatrix}, \quad \mathbf{A}_{21} = \begin{bmatrix} \xi \rho \\ 0 \end{bmatrix},$$

$$\mathbf{A}_{22} = \begin{bmatrix} u_{11} & 0 \\ u_{21} & u_{22} \end{bmatrix}.$$

$$u_{11} = \frac{\dot{S}}{S} - \frac{\dot{E}}{E} - \eta_1 I - \eta_2 \phi A - \eta_3 qH - \varpi_0,$$

$$u_{21} = \eta_1 I - \eta_2 \phi A - \eta_3 qH - \eta_4 C,$$

$$u_{22} = \frac{\dot{S}}{S} - \frac{\dot{E}}{E} - \xi - 2\varpi_0.$$

Let (n_1, n_2, n_3) be vector in R^3 and $\|\cdot\|$ of (n_1, n_2, n_3) presented by,

$$\|(n_1, n_2, n_3)\| = \max\{\|n_1\|, \|n_2\| + \|n_3\|\}. \quad (4.10)$$

Here we consider the Lozinski-measure introduced in [41], $\delta(\mathbf{A}) \leq \sup\{\varrho_1, \varrho_2\} = \sup\{\delta(\mathbf{A}_{11}) + \|\mathbf{A}_{12}\|, \delta(\mathbf{A}_{22}) + \|\mathbf{A}_{21}\|\}$, where $h_i = \delta(\mathbf{A}_{ii}) + \|\mathbf{A}_{ij}\|$ for $i = 1, 2$ and $i \neq j$, \Rightarrow

$$\varrho_1 = \delta(\mathbf{A}_{11}) + \|\mathbf{A}_{12}\|, \quad \varrho_2 = \delta(\mathbf{A}_{22}) + \|\mathbf{A}_{21}\|, \quad (4.11)$$

where $\delta(\mathbf{A}_{11}) = \frac{\dot{S}}{S} - \frac{\dot{E}}{E} - \eta_1 I - \eta_2 \phi A - \eta_3 q H - (\xi + \varpi_0)$, $\delta(\mathbf{A}_{22}) = \max\left\{\frac{\dot{S}}{S} - \frac{\dot{E}}{E} - \eta_1 I - \eta_2 \phi A - \eta_3 q H - \varpi_0, \eta_1 I - \eta_2 \phi A - \eta_3 q H - \eta_4 C\right\}$, $\|\mathbf{A}_{12}\| = \eta_1 S$ and $\|\mathbf{A}_{21}\| = \max\{\xi\rho, 0\} = \xi\rho$. Therefore ϱ_1 and ϱ_2 become, i.e., $\varrho_1 \leq \frac{\dot{S}}{S} - 2\varpi_0 - \xi\rho$ and $\varrho_2 \leq \frac{\dot{S}}{S} - 2\varpi_0 - \xi - \min\{\sigma_1, \nu\rho\}$, which presents $\delta(\mathbf{A}) \leq \left\{\frac{\dot{S}}{S} + \sigma_1 - \min\{\xi, \sigma_1\} - 2\varpi_0\right\}$. Hence $\delta(B) \leq \frac{\dot{S}}{S} - 2\varpi_0$. Integrating $\delta(\mathbf{A})$ in $[0, t]$ and also considering $\lim_{t \rightarrow \infty}$, we have

$$\limsup_{t \rightarrow \infty} \sup \frac{1}{t} \int_0^t \delta(\mathbf{A}) dt < -2\varpi_0, \quad (4.12)$$

$$\bar{k} = \limsup_{t \rightarrow \infty} \sup \frac{1}{t} \int_0^t \delta(\mathbf{A}) dt < 0.$$

So that the system of the first three compartments of model (2.1) is globally asymptotically stable. \square

4.3. Sensitivity analysis

To find the relation of parameters to \mathcal{R}_0 in the disease transmission we use the formula $\Delta_h^{\mathcal{R}_0} = \frac{\partial \mathcal{R}_0}{\partial h} \frac{h}{\mathcal{R}_0}$ where h is the parameter, introduced by [34, 35]. This makes it easy to identify the variables that have a substantial impact on reproduction number, using the above formula we have

$$\begin{aligned} \Delta_{\eta_1}^{\mathcal{R}_0} &= \frac{\partial \mathcal{R}_0}{\partial \eta_1} \frac{\eta_1}{\mathcal{R}_0} = 0.60143 > 0, & \Delta_{\eta_2}^{\mathcal{R}_0} &= \frac{\partial \mathcal{R}_0}{\partial \eta_2} \frac{\eta_2}{\mathcal{R}_0} = 0.0020302 > 0, \\ \Delta_{\eta_3}^{\mathcal{R}_0} &= \frac{\partial \mathcal{R}_0}{\partial \eta_3} \frac{\eta_3}{\mathcal{R}_0} = 0.083624 > 0, & \Delta_{\eta_4}^{\mathcal{R}_0} &= \frac{\partial \mathcal{R}_0}{\partial \eta_4} \frac{\eta_4}{\mathcal{R}_0} = 0.90820 > 0, \\ \Delta_{\xi}^{\mathcal{R}_0} &= \frac{\partial \mathcal{R}_0}{\partial \xi} \frac{\xi}{\mathcal{R}_0} = 0.130434 > 0, & \Delta_{\varpi_2}^{\mathcal{R}_0} &= \frac{\partial \mathcal{R}_0}{\partial \varpi_2} \frac{\varpi_2}{\mathcal{R}_0} = -1.002654 < 0, \\ \Delta_{\varpi_0}^{\mathcal{R}_0} &= \frac{\partial \mathcal{R}_0}{\partial \varpi_0} \frac{\varpi_0}{\mathcal{R}_0} = -1.33673 < 0, & \Delta_{\varpi_1}^{\mathcal{R}_0} &= \frac{\partial \mathcal{R}_0}{\partial \varpi_1} \frac{\varpi_1}{\mathcal{R}_0} = 0.0043 > 0, \\ \Delta_{\psi_1}^{\mathcal{R}_0} &= \frac{\partial \mathcal{R}_0}{\partial \psi_1} \frac{\psi_1}{\mathcal{R}_0} = 0.006549 > 0, & \Delta_{\phi}^{\mathcal{R}_0} &= \frac{\partial \mathcal{R}_0}{\partial \phi} \frac{\phi}{\mathcal{R}_0} = .9999999997 > 0, \\ \Delta_{\psi_2}^{\mathcal{R}_0} &= \frac{\partial \mathcal{R}_0}{\partial \psi_2} \frac{\psi_2}{\mathcal{R}_0} = 0.996194 > 0, & \Delta_{\nu}^{\mathcal{R}_0} &= \frac{\partial \mathcal{R}_0}{\partial \nu} \frac{\nu}{\mathcal{R}_0} = -0.843190 < 0, \\ \Delta_{\sigma_1}^{\mathcal{R}_0} &= \frac{\partial \mathcal{R}_0}{\partial \sigma_1} \frac{\sigma_1}{\mathcal{R}_0} = -0.012374 < 0, & \Delta_{\sigma_2}^{\mathcal{R}_0} &= \frac{\partial \mathcal{R}_0}{\partial \sigma_2} \frac{\sigma_2}{\mathcal{R}_0} = -0.00773 < 0. \end{aligned}$$

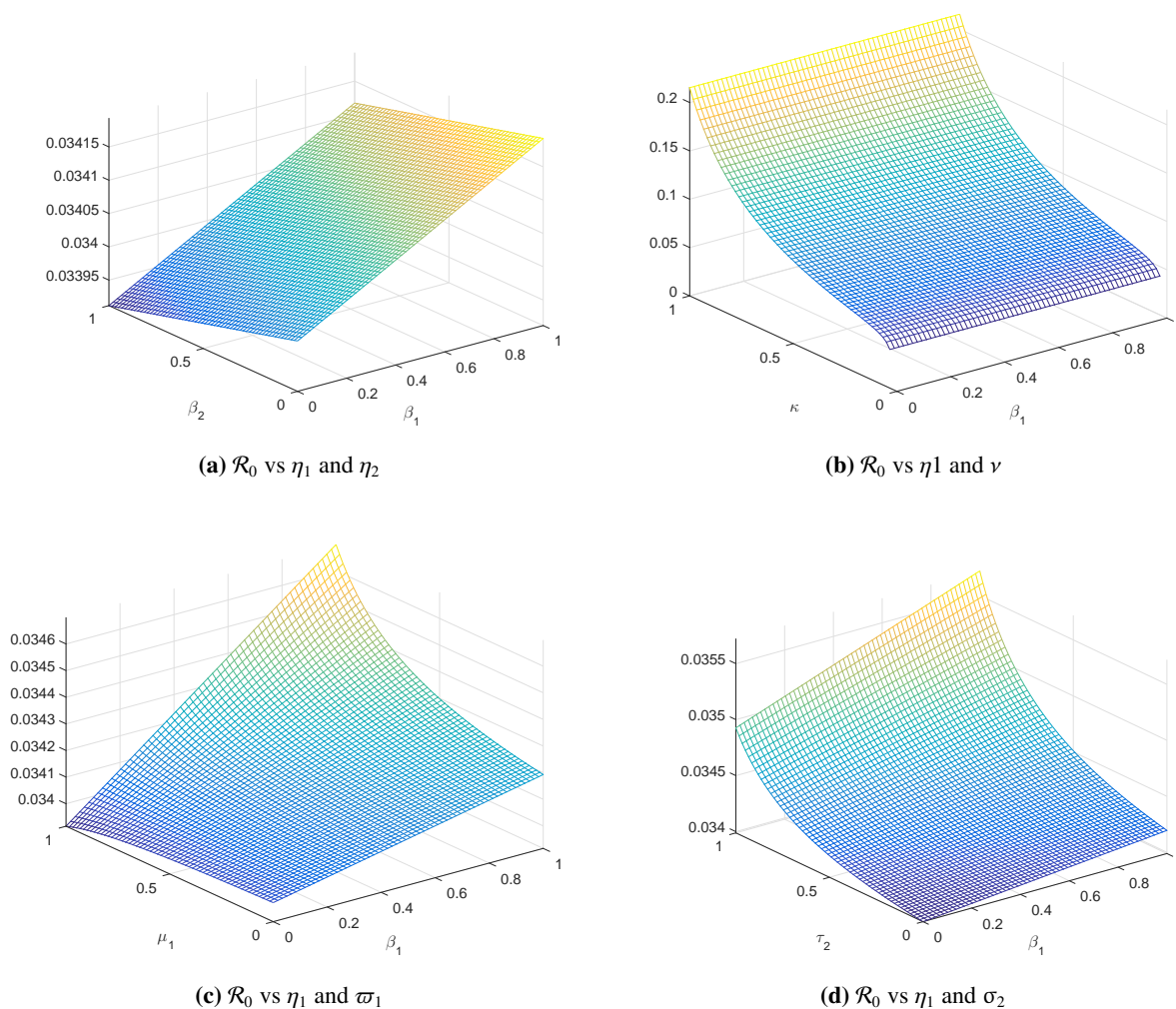


Figure 1. The graphs show the affect of various parameters on \mathcal{R}_0 and the variations in them.

These demonstrate the relevance of many factors in disease transmission. It also measures the change in \mathcal{R}_0 as a function of a parameter modification. The sensitivity indices show that there is indeed a direct relationship between \mathcal{R}_0 and a set of variables $S_1 = [\eta_1, \eta_2, \eta_3, \eta_4, \phi, \psi_1, \psi_2]$, while has an inverse relation with $S_2 = [\varpi_0, \varpi_2, \sigma_1, \sigma_2, \nu]$. This demonstrates that higher the value of parameters S_1 increases the value of threshold quantity greatly, but increasing the value for parameters S_2 decreases the value of threshold value.

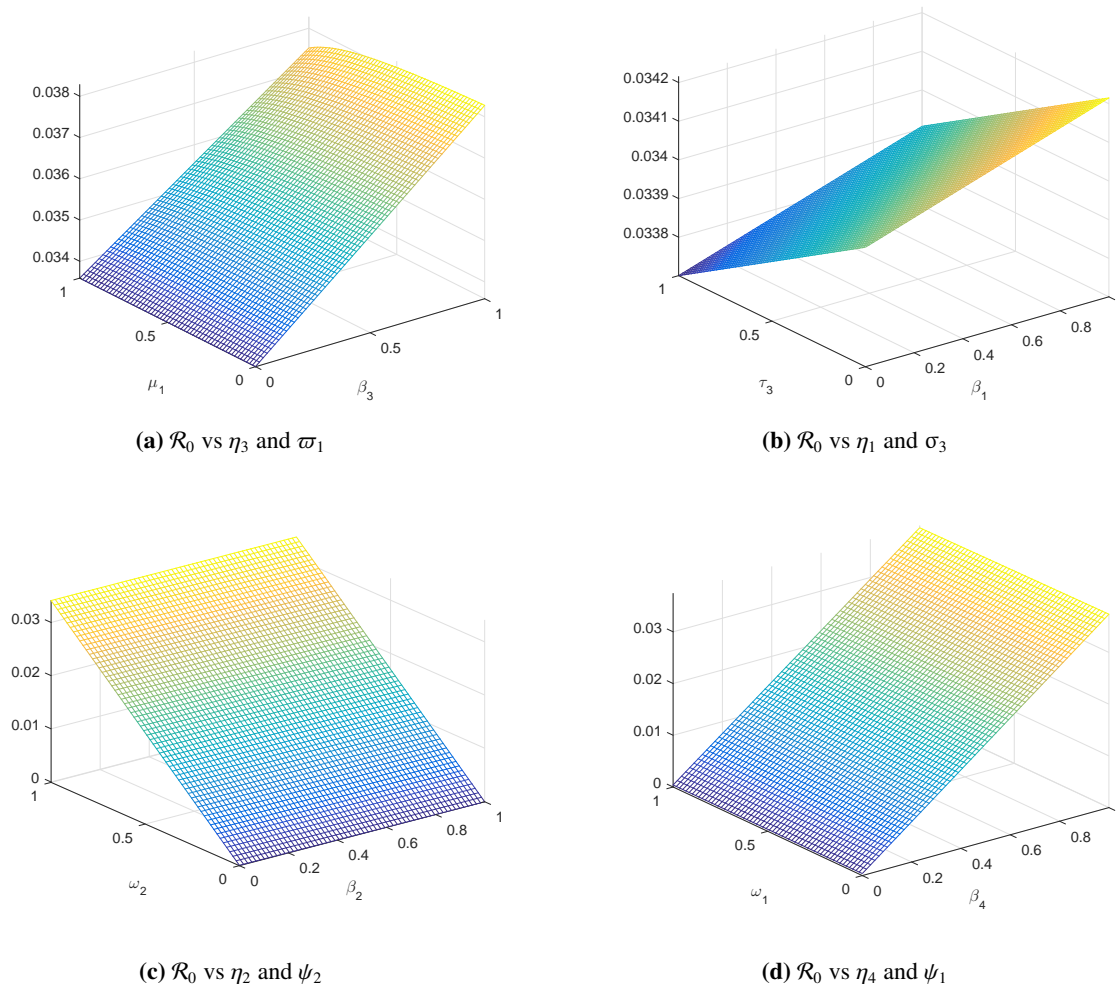


Figure 2. The graphs show the affect of various parameters on \mathcal{R}_0 and the variations in them.

5. Numerical simulation

In this part, we validate our analytical conclusion. We employ the Runge-Kutta technique of fourth order [42]. Some factors are chosen for demonstration purposes, while others are derived from publicly available data. The parameters are chosen in a way that is more biologically realistic. For the simulation, we use the following parameters. $\phi = 0.00004$; $\eta_1 = 0.007$; $\varpi_0 = 0.0003$; $\eta_2 = 0.003$; $\psi_2 = 0.00008$; $\varpi_1 = 0.0001$; $\eta_3 = 0.005$; $\xi = 0.002$; $\eta_4 = 0.0001$; $\sigma_2 = 0.000001$; $\phi = 0.016$; $q = 0.00007$; $\varpi_2 = 0.00003$; $\sigma_1 = 0.001$; $\sigma_3 = 0.0007$; $\psi_1 = 0.0006$; $\nu = 0.000002$. Figures 3 and 4 depict the performance of the proposed model based on the aforementioned parameters, which validate the theorem's analytical discovery (6). According to the theoretical understanding of these findings, whenever $R_0 < 1$, each curve of solution of the sensitive population takes 150–300 days to achieve equilibrium. Likewise, the exposed community takes 250 to 150 days, the infected populace takes 200 to 100 days, and the asymptomatic populace, hospitalized, and recovered requires 100 to 50 days. Camel dynamics initially grow and then achieve an equilibrium state, as seen in illustration 0.

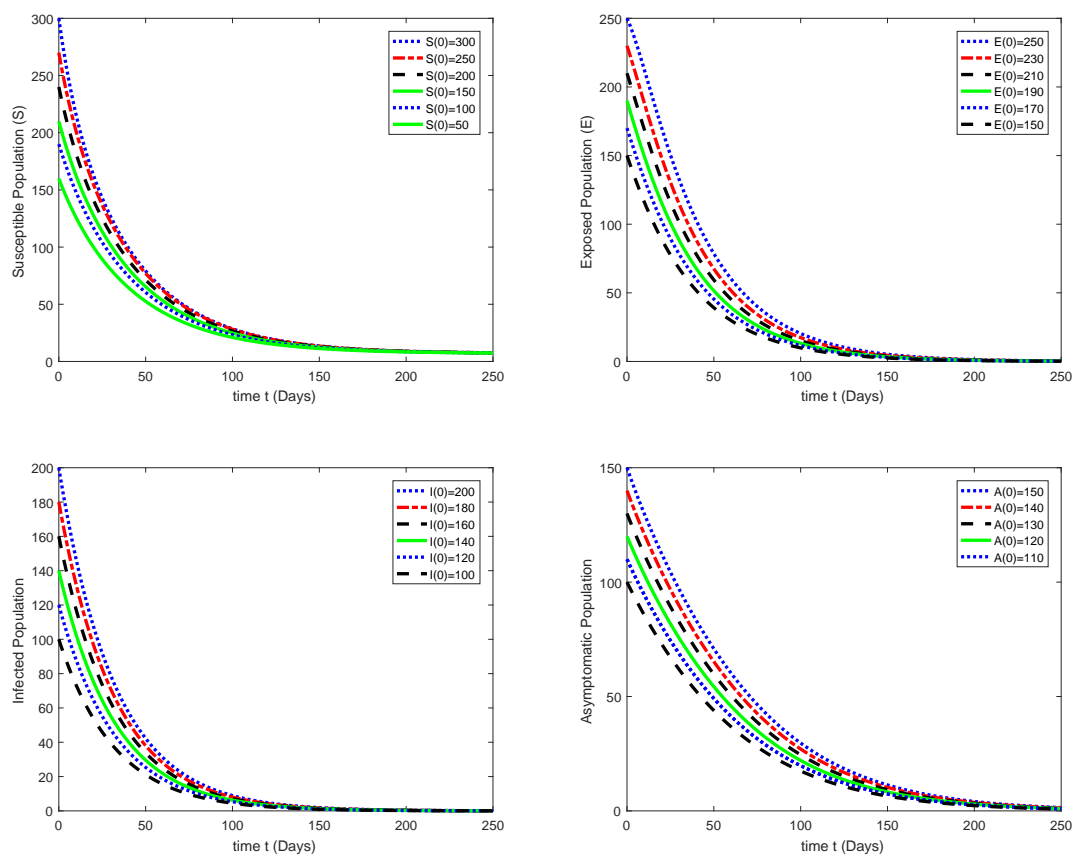


Figure 3. The demonstration of dynamics of S, I, E, A compartments population in case $\mathcal{R}_0 < 1$.

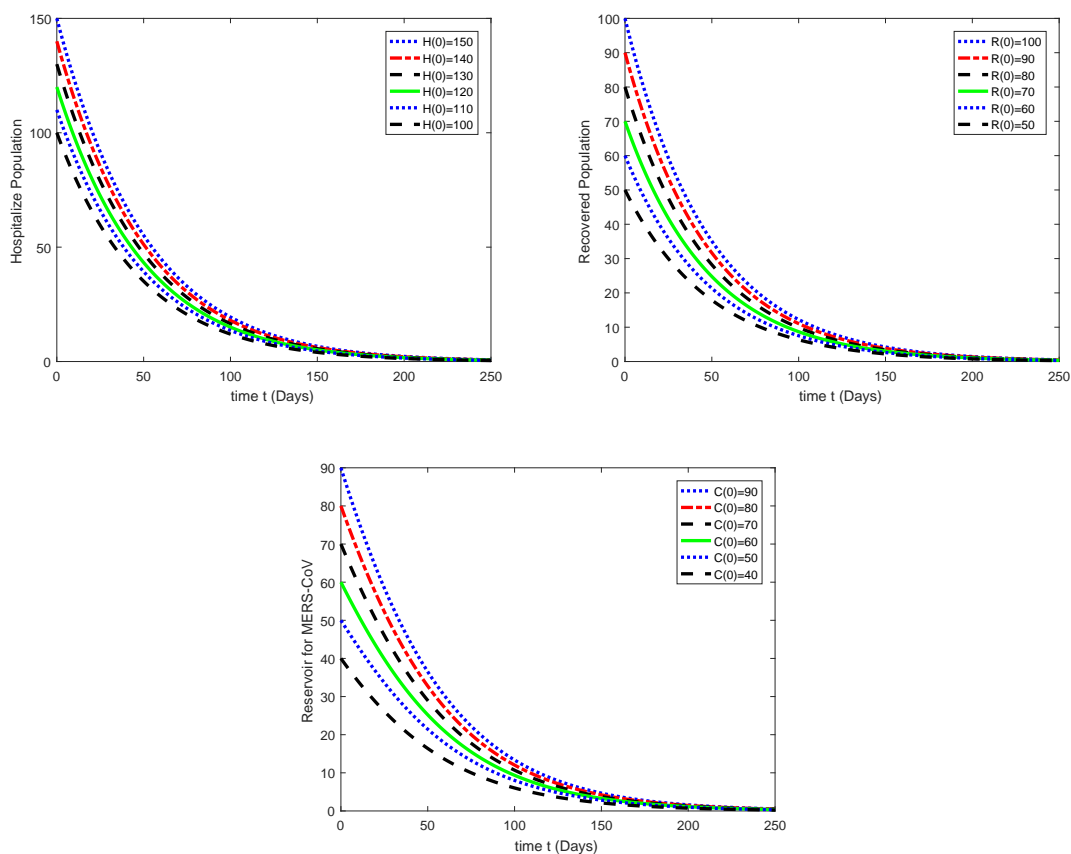


Figure 4. The demonstration of dynamics of various compartments populations (Hospitalized individuals, Recovered population, and Reservoir (MERS CoV), such that camel's in case $\mathcal{R}_0 < 1$).

Next, we consider the parameters $\eta_1 = 0.007$; $\sigma_1 = 0.001$; $\varpi_1 = 0.0001$; $\psi_1 = 0.0006$; $\eta_2 = 0.003$; $\varpi_2 = 0.00003$; $\phi = 0.00004$; $\sigma_2 = 0.000001$; $\eta_3 = 0.005$; $\varpi_0 = 0.0003$; $\eta_4 = 0.0001$; $\xi = 0.002$; $\phi = 0.016$; $\sigma_3 = 0.0007$; $q = 0.00007$; $\nu = 0.000002$. $\psi_2 = 0.00008$; and find $\mathcal{R}_0 = 9.89887$ which is greater than 1. We investigate the dynamics of the given model in the vicinity of the EE point. The numerical simulations based on the aforementioned settings are displayed in Figures (5) and (6), which validate the finding presented in Theorem (8).

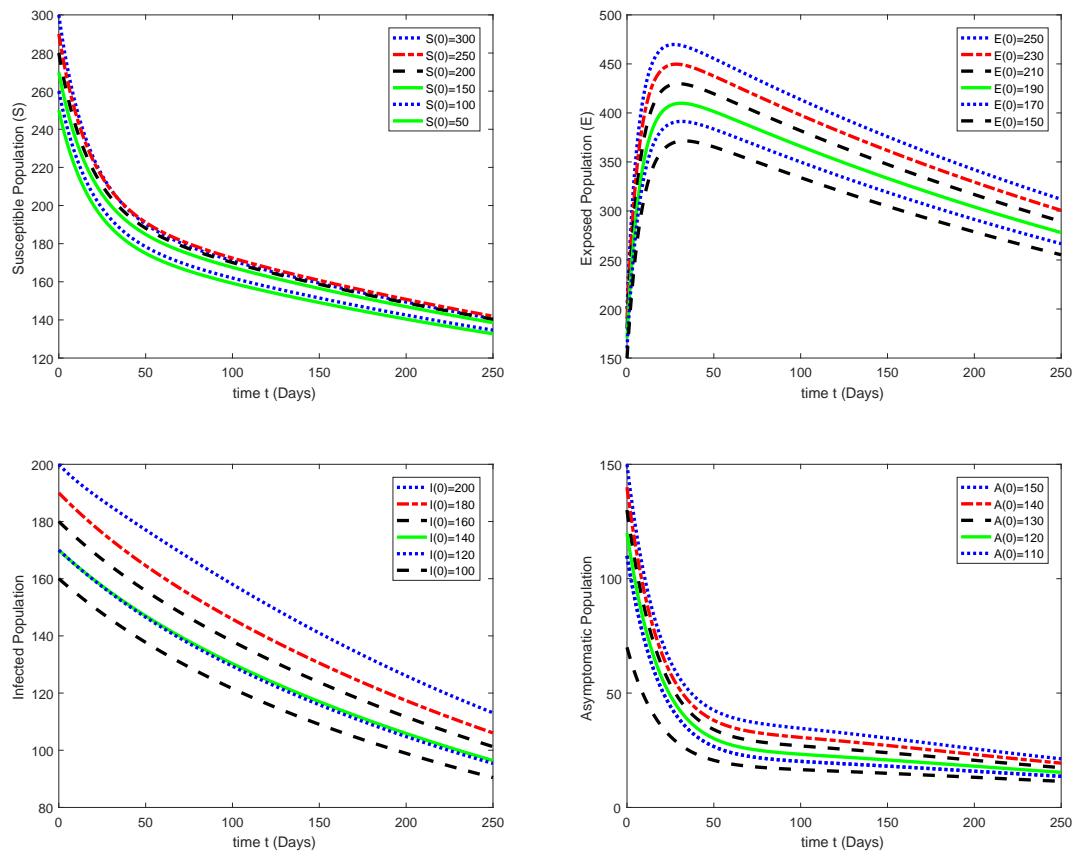


Figure 5. The demonstration of dynamics of S, I, E, A compartments populations in case $\mathcal{R}_0 > 1$.

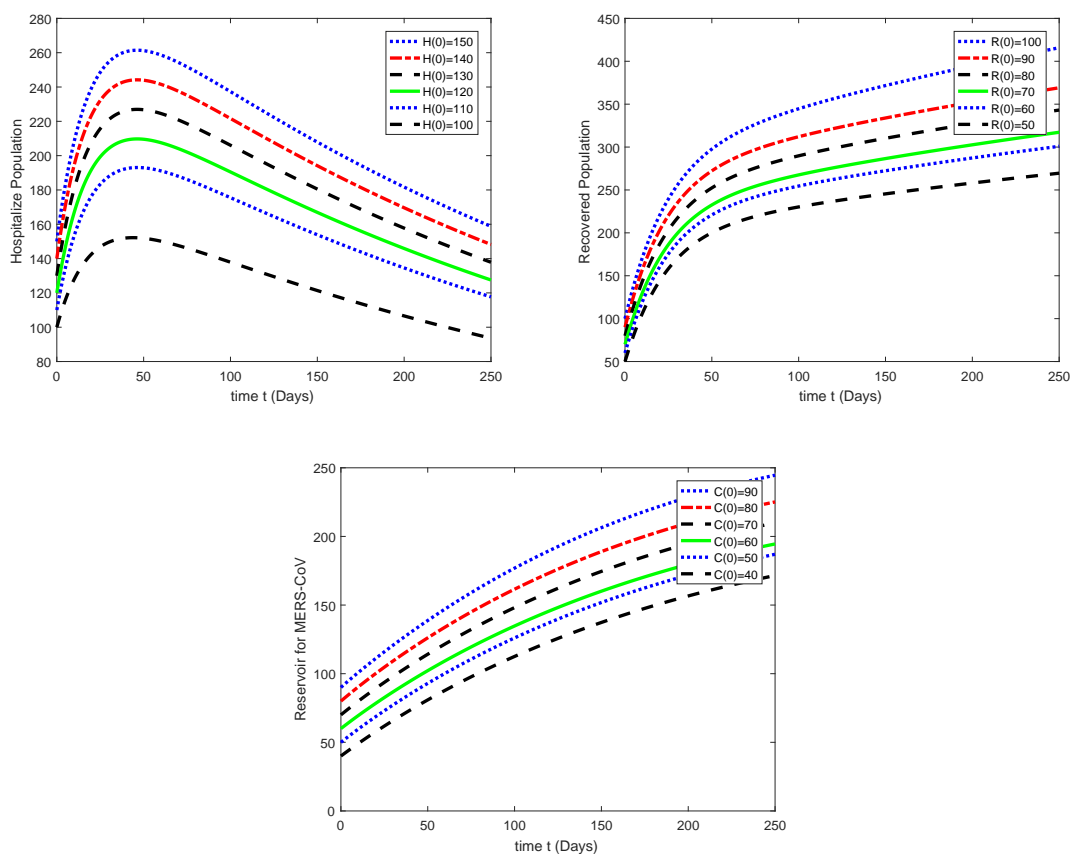


Figure 6. The demonstration of dynamics of various compartments population (Hospitalized individuals, Recovered populace, and (MERS CoV) reservoir, such that camel's in case $\mathcal{R}_0 > 1$).

6. Optimal control (OC) strategy for the reduction of infected with MERS-CoV

We develop control techniques based on sensitivity as well as model dynamics (2.1). The maximal sensitivity indices parameter is $(\eta_1, \eta_2, \eta_3, \eta_4)$, and increasing this value by 10 percent, raises the threshold value. To limit the progress of the illness, we must minimize these parameters by using the control variables $E_1(t), E_2(t), E_3(t), E_4(t)$ to represent (awareness about the mask, isolation people (infected), oxygen therapies, ventilation and self-care from the camels.)

Our main goals are the reduction of MERS-CoV in the populace with increasing $R(t)$ and decreasing $I(t)$, $A(t)$ and $H(t)$, reservoir $C(t)$ with applying control parameters (time-dependent) $E_1(t), E_2(t), E_3(t), E_4(t)$.

i. $E_1(t)$ represents the control parameter (time-dependent) represents the awareness concerning surgical masks and hand washing.

ii. $E_2(t)$ represents the control parameter (time-dependent) represents quarantining of infected persons.

iii. $E_3(t)$ represents the control parameter (time-dependent) represents mechanical ventilation (oxygen therapy).

iv. $E_4(t)$ represents the control parameter (time-dependent) self-care that is keeping distance from camels, avoiding raw milk, or eating improperly cooked meat.

By the use of these control parameters in our suggested optimal control problem which we obtain by modifying model (2.1):

$$\begin{aligned}
 \frac{dS(t)}{dt} &= \phi - \eta_1 IS(1 - E_1(t)) - \eta_2 \phi AS(1 - E_1(t)) - \eta_3 qHS(1 - E_1(t)) \\
 &\quad - \eta_4 CS(1 - E_1(t)) - \varpi_0 S, \\
 \frac{dE(t)}{dt} &= \eta_1 IS(1 - E_1(t)) + \eta_2 \phi AS(1 - E_1(t)) + \eta_3 qHS(1 - E_1(t)) + \eta_4 CS(1 - E_1(t)) \\
 &\quad - (\xi + \varpi_0 + E_1(t))E, \\
 \frac{dI(t)}{dt} &= \xi \rho E - (\sigma_1 + \sigma_2)I - (\varpi_0 + \varpi_1)I - E_2(t)I, \\
 \frac{dA(t)}{dt} &= \xi E(1 - \rho) - (\nu + \varpi_0)A - E_2(t)A, \\
 \frac{dH(t)}{dt} &= \sigma_1 I + \nu A - (\sigma_3 + \varpi_0)H - E_3(t)H, \\
 \frac{dR(t)}{dt} &= \sigma_1 IE_2(t) + \sigma_3 HE_3(t) - \varpi_0 R, \\
 \frac{dC(t)}{dt} &= \psi_1 I + \psi_2 A - \varpi_2 C(t) - E_4(t)C(t),
 \end{aligned} \tag{6.1}$$

with the initial conditions

$$I_{cs} = \{S(0), I(0), E(0), H(0), A(0), C(0), R(0)\} \geq 0$$

The purpose here is to demonstrate that it is feasible to apply time-dependent control mechanisms while reducing the expense of doing so. We assume that the expenses of control schemes are nonlinear and take a quadratic shape, [43], which are cost variables that balance the size and importance of the sections of the optimization problem. As a result, we select the observable (cost) function as,

$$J(\mathbb{E}_1, \mathbb{E}_2, \mathbb{E}_3, \mathbb{E}_4) = \int_0^T [\zeta_1 I + \zeta_2 A + \zeta_3 H + \zeta_4 C + \frac{1}{2}(\zeta_5 \mathbb{E}_1^2(t) + \zeta_6 \mathbb{E}_2^2(t) + \zeta_7 \mathbb{E}_3^2(t) + \zeta_8 \mathbb{E}_4^2(t))] dt. \quad (6.2)$$

In Eq (6.2) $\zeta_1, \zeta_2, \zeta_3, \zeta_4, \zeta_5, \zeta_6, \zeta_7, \zeta_8$, stand for weight constants. $\zeta_1, \zeta_2, \zeta_3, \zeta_4$ express relative costs of infected (I), asymptomatic (A), hospitalized (H) and reservoir (C), while $\zeta_5, \zeta_6, \zeta_7, \zeta_8$ show associated-cost of control parameters. $\frac{1}{2}\zeta_5 \mathbb{E}_1^2, \frac{1}{2}\zeta_8 \mathbb{E}_4^2, \frac{1}{2}\zeta_6 \mathbb{E}_2^2, \frac{1}{2}\zeta_7 \mathbb{E}_3^2$, describe self care, treatment and isolation.

Our objective is to obtain OC pair $\mathbb{E}_1^*, \mathbb{E}_2^*, \mathbb{E}_3^*, \mathbb{E}_4^*$, i.e.,

$$J(\mathbb{E}_1^*, \mathbb{E}_2^*, \mathbb{E}_3^*, \mathbb{E}_4^*) = \min\{J(\mathbb{E}_1, \mathbb{E}_2, \mathbb{E}_3, \mathbb{E}_4), \mathbb{E}_1, \mathbb{E}_2, \mathbb{E}_3, \mathbb{E}_4 \in U\}, \quad (6.3)$$

dependent on model (6.1), we consider, the control-set of parameters as:

$$U = \{(\mathbb{E}_1, \mathbb{E}_2, \mathbb{E}_3, \mathbb{E}_4)/u_i(t) \text{ is Lebesgue-measurable on the } [0, 1], 0 \leq u_i(t) \leq 1, i = 1, 2, 3, 4\}. \quad (6.4)$$

We obey the result [44], stating that the solution of the system exists in the case when control parameters are bounded as well as Lebesgue measurable. So, we consider that the suggested control system can be presented as:

$$\frac{d\Omega}{dt} = A\Omega + \mathcal{B}\Omega.$$

In above system $\Omega = (S, I, E, H, A, C)$, $A(\Omega)$ and $\mathcal{B}(\Omega)$ represent linear and nonlinear bounded coefficient, respectively, so that

$$A = \begin{bmatrix} -\varpi_0 & 0 & 0 & 0 & 0 & 0 \\ 0 & -y_1 & 0 & 0 & 0 & 0 \\ 0 & \nu\rho & -y_2 & 0 & 0 & 0 \\ 0 & \nu(-\rho + 1) & 0 & -y_3 & 0 & 0 \\ 0 & 0 & \sigma_1 & \epsilon & -(\sigma_2 + \varpi_0 + \mathbb{E}_3) & 0 \\ 0 & 0 & \psi_1 & \psi_2 & 0 & -(\theta + \mathbb{E}_4) \end{bmatrix}, \quad (6.5)$$

where $y_1 = (\nu + \varpi_0 + \mathbb{E}_1)$, $y_2 = (\sigma_1 + \sigma_2 + \varpi_0 + \varpi_1 + \mathbb{E}_2)$, $y_3 = (\epsilon + \varpi_0 + \varpi_2 + \mathbb{E}_2)$.

$$B(\Omega) = \begin{pmatrix} \phi - \eta_1 IS(1 - \mathbb{E}_1(t)) - \eta\theta A\phi S(1 - \mathbb{E}_1(t)) - \eta_3 qHS(1 - \mathbb{E}_1(t)) - \eta_4 CS(1 - \mathbb{E}_1(t)) \\ \eta_1 IS(1 - \mathbb{E}_1(t)) + \eta_2 \phi AS(1 - \mathbb{E}_1(t)) + \eta_3 qHS(1 - \mathbb{E}_1(t)) + \eta_4 CS(1 - \mathbb{E}_1(t)) \\ 0 \\ 0 \\ 0 \\ 0 \end{pmatrix}.$$

Considering $L(\Omega) = F\Omega + A\Omega$,

$$|F(\Omega_1) - F(\Omega_2)| \leq p_1|S_1 - S_2| + p_2|E_1 - E_2| + p_3|I_1 - I_2| + p_4|A_1 - A_2|$$

$$\begin{aligned}
& + p_5|H_1 - H_2| + p_6|C_1 - C_2| \\
& \leq P|S_1 - S_2| + |E_1 - E_2| + |C_1 - C_2| + |I_1 - I_2| \\
& + |H_1 - H_2| + |A_1 - A_2|.
\end{aligned}$$

Here $P = \max(p_1, p_2, p_3, p_4, p_5, p_6, p_7, p_8)$ does not depend on the suggested model state-classes. We can also express

$$|L(\Omega_1) - L(\Omega_2)| \leq |W(\Omega_1) - W(\Omega_2)|,$$

where $W = (P, \|A\|)$ is less than ∞ , L is continuous in the Lipschitz sense, and from the description the system classes are non-negative, it obviously shows that the solution of model (6.1) exists. For the existence of the solution let us consider, and prove the following theorem:

Theorem 10. *There exist an OC $E^* = (E_1^*, E_2^*, E_3^*, E_4^*) \in E$, to control-system presented in Eqs (6.1) and (6.2).*

Proof. As it is obvious that the control and system variables are not negative. It is also worth noting that U (set of variables) is closed and convex by expression. Furthermore, the control problem is bounded, indicating the problem's compactness. The expression $\zeta_1 I + \zeta_2 A + \zeta_3 H + \zeta_4 C + \frac{1}{2}(\zeta_5 E_1^2(t) + \zeta_6 E_2^2(t) + \zeta_7 E_3^2(t) + \zeta_8 E_4^2(t))$ is convex as well, w.r.t the set U . It guarantees the existence of OC for OC variables $(E_1^*, E_2^*, E_3^*, E_4^*)$. \square

6.1. Methods

Here, we determine the best solution to control problems (6.1) and (6.2). For this, we employ the Lagrangian, and Hamiltonian equations, as shown below:

$$L(I, C, A, H, E_1, E_2, E_3, E_4) = \zeta_1 I + \zeta_2 A + \zeta_3 H + \zeta_4 C + \frac{1}{2}(\zeta_5 E_1^2(t) + \zeta_6 E_2^2(t) + \zeta_7 E_3^2(t) + \zeta_8 E_4^2(t)).$$

To define the Hamiltonian (H) associated with the model, we use the notion $\Theta = (\Theta_1, \Theta_2, \Theta_3, \Theta_4, \Theta_5, \Theta_6, \Theta_7)$ and $\Upsilon = (\Upsilon_1, \Upsilon_2, \Upsilon_3, \Upsilon_4, \Upsilon_5, \Upsilon_6, \Upsilon_7)$ then,

$$H(x, u, \Theta) = L(x, u) + \Theta \Upsilon(x, u),$$

where

$$\begin{aligned}
\Upsilon_1(x, u) &= \phi - \eta_1 IS(1 - E_1(t)) - \eta_2 \phi AS(1 - E_1(t)) - \eta_3 qHS(1 - E_1(t)) \\
&\quad - \eta_4 CS(1 - E_2(t)) - \varpi_0 S, \\
\Upsilon_2(x, u) &= \eta_1 IS(1 - E_1(t)) + \eta_2 \phi AS(1 - E_1(t)) + \eta_3 qHS(1 - E_1(t)) + \eta_4 CS(1 - E_2(t)) \\
&\quad - (\xi + \varpi_0 + E_1)E, \\
\Upsilon_3(x, u) &= \xi \rho E - (\sigma_1 + \sigma_2)I - (\varpi_0 + \varpi_1)I - E_2(t)I(t), \\
\Upsilon_4(x, u) &= \xi(1 - \rho)E - (\nu + \varpi_0)A - E_2(t)A, \\
\Upsilon_5(x, u) &= \sigma_1 I + \nu A - (\sigma_3 + \varpi_0)H - E_3(t)H, \\
\Upsilon_6(x, u) &= \sigma_1 IE_2(t) + \sigma_3 HE_3(t) - \varpi_0 R, \\
\Upsilon_7(x, u) &= \psi_1 I + \psi_2 A - \varpi_2 C - E_4(t)C(t),
\end{aligned} \tag{6.6}$$

and $\mathfrak{Z}(x, u) = \Upsilon_1(x, u), \Upsilon_2(x, u), \Upsilon_3(x, u), \Upsilon_4(x, u), \Upsilon_5(x, u), \Upsilon_6(x, u), \Upsilon_7(x, u)$.

Here we utilize, the principle [45, 46] to Hamiltonian, in order to obtain an optimality solution, which is stated that if the solution expressed with (x^*, u^*) is optimal, then \exists a function Θ , such that

$$\dot{x} = \frac{\partial H}{\partial \Theta}, 0 = \frac{\partial H}{\partial u},$$

$$\Theta A(t)' = -\frac{\partial H}{\partial x}.$$

$$H(t, x^*, u^*, \Theta) \partial x = \max_{\mathbb{E}_1, \mathbb{E}_2, \mathbb{E}_3, \mathbb{E}_4 \in [0, 1]} H(x^*(t), \mathbb{E}_1, \mathbb{E}_2, \mathbb{E}_3, \mathbb{E}_4, \Theta A(t)); \quad (6.7)$$

and the condition of transversality

$$\Theta(t_f) = 0. \quad (6.8)$$

Thus to obtain the adjoint variables and OC variables, we use the principles Eq (6.7). So we get

Theorem 11. Suppose that optimal and control-parameters are expressed by $S^*, E^*, A^*, I^*, H^*, C^*, R^*$ be the optimal-state $(\mathbb{E}_1^*, \mathbb{E}_2^*, \mathbb{E}_3^*, \mathbb{E}_4^*)$ for system (6.1)-(6.2). Then $\Theta A(t)$ (adjoint variables set) satisfies:

$$\begin{aligned} \Theta_1'(t) &= (\Theta_1 - \Theta_2)(\eta_1 I^* + \eta_2 \phi A^* + \eta_3 q H^* + \eta_4 C^*)(1 - \mathbb{E}_1(t)) + \Theta_1 \varpi_0, \\ \Theta_2'(t) &= (\Theta_2 - \Theta_4)\xi + (\Theta_4 - \Theta_3)\xi \rho + \Theta_2 \varpi_0 + \Theta_2 \mathbb{E}_1(t), \\ \Theta_3'(t) &= \zeta_1 + (\Theta_1 - \Theta_2)\eta_1 S^*(1 - \mathbb{E}_1(t)) + (\Theta_3 - \Theta_5)\sigma_1 - \Theta_6 \xi_1 \mathbb{E}_2(t) - \Theta_7 \\ \Theta_4'(t) &= -\zeta_2 + (\Theta_1 - \Theta_2)\eta_2 \phi S^*(1 - \mathbb{E}_1(t)) + (\Theta_4 - \Theta_5)\nu + \Theta_4(\varpi_0 + \mathbb{E}_2(t)) - \Theta_7 \psi_2, \\ \Theta_5'(t) &= -\zeta_3 - (\Theta_1 - \Theta_2)\eta_3 q S^*(1 - \mathbb{E}_1(t)) + (\sigma_3 + u_0 + \mathbb{E}_3(t))\Theta_5 - \Theta_6 \sigma_3 \mathbb{E}_3(t), \\ \Theta_6'(t) &= -\varpi_0 \Theta_6, \\ \Theta_7'(t) &= -\zeta_4 + (\Theta_1 - \Theta_2)\eta_4 S^*(1 - \mathbb{E}_1(t)) + \Theta_7(\varpi_2 + \mathbb{E}_4(t)), \end{aligned} \quad (6.9)$$

having terminal condition

$$\Theta A(t) = 0. \quad (6.10)$$

The OC variables $\mathbb{E}_1^*(t), \mathbb{E}_2^*(t), \mathbb{E}_3^*(t), \mathbb{E}_4^*(t)$ are

$$\begin{aligned} \mathbb{E}_1^*(t) &= \max \left[\min \left[\frac{(\Theta_2 - \Theta_1)\eta_1 I^* S^* + \eta_2 \phi A^* + \eta_3 q H^* + \eta_4 C^* S^* + \Theta_2 E^*}{\zeta_5}, 1 \right], 0 \right], \\ \mathbb{E}_2^*(t) &= \max \left[\min \left[\frac{(\Theta_3 I^* + \Theta_6 \sigma_1 R^* + \Theta_4 A^* + \Theta_5 H^*)}{\zeta_6}, 1 \right], 0 \right], \\ \mathbb{E}_3^*(t) &= \max \left[\min \left[\frac{(\Theta_5 H^* - \Theta_6 \sigma R^*)}{\zeta_7}, 1 \right], 0 \right], \\ \mathbb{E}_4^*(t) &= \max \left[\min \left[\frac{(\Theta_7 C^*)}{\zeta_8}, 1 \right], 0 \right]. \end{aligned} \quad (6.11)$$

Proof: The adjoint-model (6.9) is obtained by applying the principle (6.7) and the transversality conditions from the outcomes of $\Theta A(t) = 0$. For optimal functions set $\mathbb{E}_1^*, \mathbb{E}_2^*, \mathbb{E}_3^*$ and \mathbb{E}_4^* , we utilized $\frac{\partial H}{\partial u}$. In the next part, we evaluate the optimality problem numerically. Since it will be easier for such readers to understand as compared to analytical data. The optimization problem system is defined by its control-system (6.1), adjoint-system (6.9), boundary conditions, and OC functions.

6.2. Numerical simulation of optimal control results

Using the RK technique of order four, we calculate the optimal control model (6.1) to observe the influence of masks, treatment, isolations, and self-care from camels. We employ the forward RK technique to get the solution of system (2.1) with starting conditions in the time interval $[0, 50]$. To obtain a solution to the adjoint-system (6.9), we apply the backward RK technique in the same domain with the assistance of the transversality constraint. For simulation purposes, we consider the parameters as: $\nu = 0.0071$; $\varpi_1 = 0.014567125$; $\eta_1 = 0.00041$; $\eta_3 = 0.0000123$; $\eta_4 = 0.0000123$; $\theta = 0.98$; $\sigma_1 = 0.0000404720925$; $\sigma_3 = 0.00135$; $q = 0.017816$; $\psi_1 = 0.05$; $\varpi_0 = 0.00997$; $\eta_2 = 0.0000123$; $\phi = 0.003907997$; $\sigma_2 = 0.000431$; $\rho = 0.00007$; $\varpi_2 = 0.014567125$; $\psi_2 = 0.06$. These parameters are considered in such a manner that more feasible biologically. Weight constants, here are taken as $\zeta_1 = 0.6610000$; $\zeta_2 = 0.54450$; $\zeta_3 = 0.0090030$; $\zeta_4 = 0.44440$; $\zeta_6 = 0.3550$; $\zeta_7 = 0.67676$; $\zeta_8 = 0.999$. So we get the upcoming behaviours shown in Figures 7a,7b,7c,7d,8a,8b,8c.

These figures reflect the dynamics of susceptibles, exposed, infected people, asymptomatic persons, hospitalized, recovered, and MERS reservoirs, i.e., camels with and also without control. Our major goal in using the OC tool is to reduce the number of persons who are infected while increasing the number of those who are not infected, as demonstrated by numerical findings.

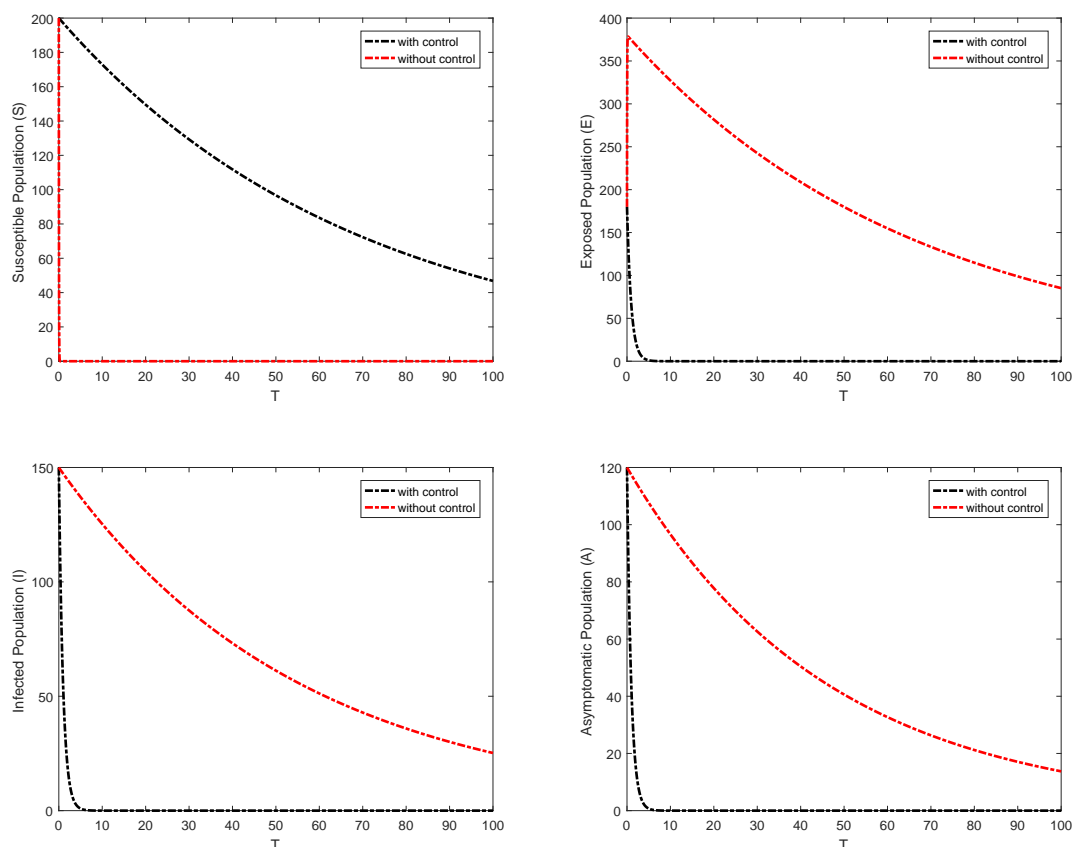


Figure 7. The graphs depict the dynamic of the classes with control and without controls.

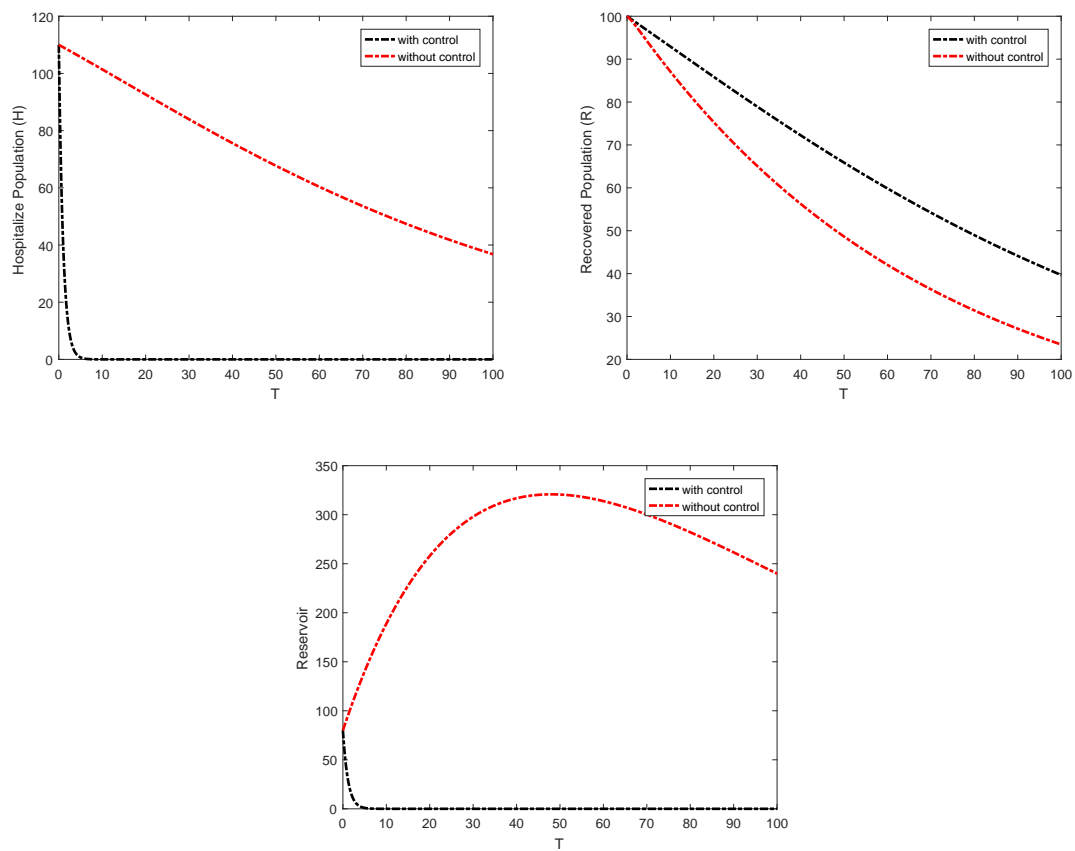


Figure 8. The graphs depict the dynamic of the classes with control and without controls.

7. Conclusions

In this study, we developed a mathematical model to analyze the transmission of MERS-CoV between people and its reservoir (camels), with the goal of assessing the transmission risk of MERS-CoV. We calculated the model's fundamental reproductive number, \mathcal{R}_0 , and employed stability theory to examine the local and global behavior of the model and determine the conditions that lead to stability. We also evaluated the sensitivity of \mathcal{R}_0 to understand the impact of each epidemiological parameter on disease transmission. To minimize the number of infected individuals and intervention costs, we incorporated optimal control into the model, which included time-dependent control variables such as supportive care, surgical masks, treatment, and public awareness campaigns about the use of masks. Furthermore, our biological interpretation of the results indicates that if the basic reproduction number is less than one, the susceptible population decreases for up to 60 days, and then becomes stable, indicating that the population will remain stable. Our numerical simulations validated the effectiveness of our control strategies in reducing the number of infected individuals, asymptomatic cases, hospitalizations, and MERS-CoV reservoir, while increasing the susceptible and recovered populations. These simulations support our analytical work.

Acknowledgement

This study is supported via funding from Prince Sattam bin Abdulaziz University project number PSAU/2023/R/1444.

References

1. E. I. Azhar, S. A. El-Kafrawy, S. A. Farraj, A. M. Hassan, M. S. Al-Saeed, A. M. Hashem, et al., Evidence for camel-to-human transmission of MERS coronavirus, *New Eng. J. Med.*, **370** (2014), 2499–2505. <https://doi.org/10.1056/NEJMoa1401505>
2. World Health Organization, Novel Coronavirus—China, Disease outbreak news: Update. Available from: <https://www.who.int/csr/don/12-january-2020-novel-coronavirus-china/en/>.
3. J. A. Al-Tawfiq, K. Hinedi, J. Ghandour, H. Khairalla, S. Musleh, A. Ujayli, et al., Middle East respiratory syndrome coronavirus: a case-control study of hospitalized patients, *Clin. Infect. Dis.*, **59** (2014), 160–165.
4. Y. M. Arabi, A. A. Arifi, H. H. Balkhy, H. Najm, A. S. Aldawood, A. Ghabashi, et al., Clinical course and outcomes of critically ill patients with Middle East respiratory syndrome coronavirus infection, *Ann. Intern. Med.*, **160** (2014), 389–397. <https://doi.org/10.7326/M13-2486>
5. I. U. Haq, M. Yavuz, N. Ali, A. Akgül, A SARS-CoV-2 fractional-order mathematical model via the modified Euler method, *Math. Comput. Appl.*, **27** (2022), 82. <https://doi.org/10.3390/mca27050082>
6. H. R. Thieme, *Modelling in Population Biology*, Princeton University Press, Princeton, 2003.
7. W. O. Kermack, A. G. McKendrick, Contributions to the mathematical theory of epidemics, part 1, *Proc. R. Soc. A*, **115** (1927), 700–721. <https://doi.org/10.1098/rspa.1927.0118>

8. Y. Kim, S. Lee, C. Chu, S. Choe, S. Hong, Y. Shin, The characteristics of Middle Eastern respiratory syndrome coronavirus transmission dynamics in South Korea, *Osong Public Health Res. Perspect.*, **7** (2016), 49–55.
9. A. N. Alagaili, T. Briese, N. Mishra, V. Kapoor, S. C. Sameroff, Middle East respiratory syndrome coronavirus infection in dromedary camels in Saudi Arabia, *MBio*, **5** (2014), e01002–e01014. <https://doi.org/10.1128/mBio.01002-14>
10. A. Assiri, J. A. Al-Tawfiq, A. A. Al-Rabeeah, F. A. Al-Rabiah, S. Al-Hajjar, A. Al-Barrak, et al., Epidemiological, demographic, and clinical characteristics of 47 cases of Middle East respiratory syndrome coronavirus disease from Saudi Arabia: a descriptive study, *Lancet Infect. Dis.*, **13** (2013), 752–761.
11. A. Zumla, D. S. Hui, S. Perlman, Middle East respiratory syndrome, *Lancet*, **386** (9997), 995–1007. [https://doi.org/10.1016/S0140-6736\(15\)60454-8](https://doi.org/10.1016/S0140-6736(15)60454-8)
12. C. Poletto, C. Pelat, D. Levy-Bruhl, Y. Yazdanpanah, P. Y. Boelle, V. Colizza, Assessment of the Middle East respiratory syndrome coronavirus (MERS-CoV) epidemic in the Middle East and risk of international spread using a novel maximum likelihood analysis approach, *Eurosurveillance*, **19** (2014), 20824.
13. K. Wang, W. Hao, H. Zhao, Aggregation and classification of spatial dynamics of vector-borne disease in advective heterogeneous environment, *J. Differ. Equations*, **343** (2023), 285–331. <https://doi.org/10.1016/j.jde.2022.10.013>
14. X. Ma, G. Q. Sun, Z. H. Wang, Y. M. Chu, Z. Jin, L. B. Li, Transmission dynamics of brucellosis in Jilin province, China: Effects of different control measures, *Commun. Nonlinear Sci. Numer. Simul.*, **114** (2022), 106702. <https://doi.org/10.1016/j.cnsns.2022.106702>
15. G. Q. Sun, H. T. Zhang, L. L. Chang, Z. Jin, H. Wang, S. Ruan, On the dynamics of a diffusive foot-and-mouth disease model with nonlocal infections, *SIAM J. Appl. Math.*, **82** (2022), 1587–1610. <https://doi.org/10.1137/21M1412992>
16. M. Rahman, M. Arfan, D. Baleanu, Piecewise fractional analysis of the migration effect in plant-pathogen-herbivore interactions, *Bull. Biomath.*, **1** (2023), 1–23.
17. B. Li, Z. Eskandari, Z. Avazzadeh, Dynamical behaviors of an SIR epidemic model with discrete time, *Fractal Fractional*, **6** (2022), 659. <https://doi.org/10.3390/fractalfract6110659>
18. F. Evirgen, E. Uçar, S. Uçar, N. Özdemir, Modelling Influenza A disease dynamics under Caputo-Fabrizio fractional derivative with distinct contact rates, *Math. Model. Numer. Simul. Appl.*, **3** (2023), 58–72.
19. A. G. C. Pérez, D. A. Oluyori, A model for COVID-19 and bacterial pneumonia coinfection with community-and hospital-acquired infections, *Math. Model. Numer. Simul. Appl.*, **2** (2022), 197–210.
20. X. Jiang, J. Li, B. Li, W. Yin, L. Sun, X. Chen, Bifurcation, chaos, and circuit realisation of a new four-dimensional memristor system, *Int. J. Nonlinear Sci. Numer. Simul.*, **3** (2023), 58–73.
21. B. Li, Z. Eskandari, Z. Avazzadeh, Strong resonance bifurcations for a discrete-time prey–predator model, *J. Appl. Math. Comput.*, **2023** (2023), 1–18. <https://doi.org/10.1051/mmnp/2022036>

22. H. Joshi, M. Yavuz, S. Townley, B. K. Jha, Stability analysis of a non-singular fractional-order covid-19 model with nonlinear incidence and treatment rate, *Phys. Scr.*, **98** (2023), 045216. <https://doi.org/10.1088/1402-4896/acbe7a>
23. M. Yavuz, F. Özköse, M. Susam, M. Kalidass, A new modeling of fractional-order and sensitivity analysis for Hepatitis-B disease with real data, *Fractal Fractional*, **7** (2023), 165. <https://doi.org/10.3390/fractalfract7020165>
24. P. A. Naik, Z. Eskandari, M. Yavuz, J. Zu, Complex dynamics of a discrete-time Bazykin–Berezovskaya prey-predator model with a strong Allee effect, *J. Comput. Appl. Math.*, **413** (2022), 114401.
25. F. Özköse, M. Yavuz, M. T. Şenel, R. Habbireeh, Fractional order modelling of omicron SARS-CoV-2 variant containing heart attack effect using real data from the United Kingdom, *Chaos Solitons Fractals*, **157** (2022), 111954. <https://doi.org/10.1016/j.chaos.2022.111954>
26. H. Joshi, M. Yavuz, I. Stamova, Analysis of the disturbance effect in intracellular calcium dynamic on fibroblast cells with an exponential kernel law, *Bull. Biomath.*, **1** (2023), 24–39.
27. U. K. Nwajeri, A. O. Atede, A. B. Panle, K. U. Egeonu, Malaria and cholera co-dynamic model analysis furnished with fractional-order differential equations, *Math. Model. Numer. Simul. Appl.*, **3** (2023), 33–57.
28. A. Moustafid, Set-valued analysis of anti-angiogenic therapy and radiotherapy, *Math. Model. Numer. Simul. Appl.*, **2** (2022), 187–196.
29. V. Raghavendra, P. Veerasha, Analysing the market for digital payments in India using the predator-prey model, *Int. J. Optim. Control Theor. Appl.*, **13** (2023), 104–115. <https://doi.org/10.11121/ijocta.2023.1306>
30. S. Pak, Solitary wave solutions for the RLW equation by He’s semi inverse method, *Int. J. Nonlinear Sci. Numer. Simul.*, **10** (2009), 505–508.
31. G. F. Webb, Population models structured by age, size, and spatial position, in *Structured Population Models in Biology and Epidemiology*, Springer, Berlin, Heidelberg, 2008.
32. H. Inaba, Mathematical analysis of an age-structured SIR epidemic model with vertical transmission, *Discrete Contin. Dyn. Syst. Ser. B*, **6** (2006), 69.
33. P. V. Driessche, J. Watmough, Reproduction numbers and sub-threshold endemic equilibria for compartmental models of disease transmission, *Math. Biosci.*, **180** (2002), 29–48. [https://doi.org/10.1016/S0025-5564\(02\)00108-6](https://doi.org/10.1016/S0025-5564(02)00108-6)
34. T. Khan, Z. Ullah, N. Ali, G. Zaman, Modeling and control of the hepatitis B virus spreading using an epidemic model, *Chaos Solitons Fractals*, **124** (2019), 1–9. <https://doi.org/10.1016/j.chaos.2019.04.033>
35. T. Khan, G. Zaman, M. I. Chohan, The transmission dynamic of different hepatitis B-infected individuals with the effect of hospitalization, *J. Biol. Dyn.*, **12** (2018), 611–631. <https://doi.org/10.1080/17513758.2018.1500649>
36. J. P. LaSalle, *The Stability of Dynamical System SIAM*, Philadelphia, PA, 1976. <https://doi.org/10.21236/ADA031020>

37. J. P. LaSalle, Stability of nonautonomous system, in *Brown University Providence RILEFSCHETZ Center for Dynamical Systems*, (1976), 83–90. [https://doi.org/10.1016/0362-546X\(76\)90011-0](https://doi.org/10.1016/0362-546X(76)90011-0)
38. T. Zhang, K. Wang, X. Zhang, Modeling and analyzing the transmission dynamics of HBV epidemic in Xinjiang, China, *PloS One*, **10** (2015), e0138765. <https://doi.org/10.1371/journal.pone.0138765>
39. M. Y. Li, J. S. Muldowney, A geometric approach to global-stability problems, *SIAM J. Math. Anal.*, **27** (1996), 1070–1083. <https://doi.org/10.1137/S0036141094266449>
40. C. Castillo-Chavez, S. Blower, P. van den Driessche, D. Kirschner, A. A. Yakubu, *Mathematical Approaches for Emerging and Reemerging Infectious Diseases: An Introduction*, Springer Science Business Media, 2002.
41. R. H. Martin, Logarithmic norms and projections applied to linear differential systems, *J. Math. Anal. Appl.*, **45** (1974), 432–454. [https://doi.org/10.1016/0022-247X\(74\)90084-5](https://doi.org/10.1016/0022-247X(74)90084-5)
42. T. Khan, G. Zaman, M. I. Chohan, The transmission dynamic and optimal control of acute and chronic hepatitis B, *J. Biol. Dyn.*, **11** (2017), 172–189. <https://doi.org/10.1080/17513758.2016.1256441>
43. D. Aldila, H. Padma, K. Khotimah, B. Desjwiandra, H. Tasman, Analyzing the MERS disease control strategy through an optimal control problem, *Int. J. Appl. Math. Comput. Sci.*, **28** (2018), 169–184.
44. M. Kamien, N. Schwartz, Dynamic optimization, vol. 31 of advanced textbooks in economics, *North Holl Amsterdam Neth.*, 1991.
45. S. M. Aseev, A. V. Kryazhinskii, The Pontryagin maximum principle and optimal economic growth problems, in *Proceedings of the Steklov Institute of Mathematics*, **257** (2007).
46. A. A. Lashari, G. Zaman, Global dynamics of vector-borne diseases with horizontal transmission in host population, *Comput. Math. Appl.*, **61** (2001), 745–754. <https://doi.org/10.1111/0033-3352.00148>



AIMS Press

© 2023 the Author(s), licensee AIMS Press. This is an open access article distributed under the terms of the Creative Commons Attribution License (<http://creativecommons.org/licenses/by/4.0>)